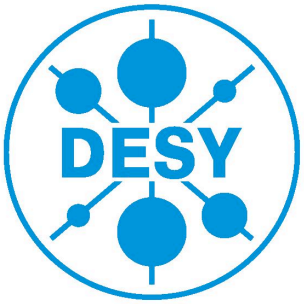

Development of a Novel Velocity Map Imaging Spectrometer

Thore Mainart Bücking, Imperial College London, United Kingdom

September 15, 2013

Abstract

A new velocity map imaging spectrometer for the recording of molecular-frame photoelectron angular distributions (MFPADs) was designed and its resolution analysed using simulations. A novel electrostatic lens design shall make 4π detection of photoelectrons with kinetic energies of up to 150 eV possible while maximising the time-of-flight difference between forward and backward emitted electrons, thus facilitating a complete 3D reconstruction of MFPADs.

Contents

1 Introduction

Molecular-frame photoelectron angular distributions (MFPADs) are potential candidates for the study of photon induced reactions on the femtosecond time scale. Here the initial momenta of photoelectrons are recorded with respect to the molecular frame. This yields information about the molecule's structure at the time of the electron emission, because the electron's wave function scatters of the other nearby nuclei, producing a diffraction pattern which is reflected in the MFPAD.
Using deep core photoionisation it is possible to cause a short lived inner shell vacancy after which the molecule decays into ionic fragments and Auger electrons. Due to the short time interval between ionisation and decay, the initially produced photoelectron can be considered to be emitted simultaneously with the ionic fragments i.e. in the same molecular frame. Hence, by measuring the ions and electrons initial momenta in coincidence, it is possible to reconstruct the MFPAD.
Using pump probe techniques it is then feasible to perform time-resolved photoelectron diffraction measurements of dissociative ionisation, making it possible to "watch chemistry in action".
The high spatial and temporal resolution needed for measurements like this can be achieved with velocity map imaging (VMI) spectroscopy. Here the initial velocities of the ions and electrons are mapped onto a multi channel plate (MCP), in such a way that fragments with the same momentum but originating from different points of and extended interaction region, for example from a supersonic molecular beam, are focused to the same spot on the MCP. This focussing of the image is known as *deblurring* and is achieved using electrostatic lensing. By using a double sided VMI spectrometer one can map ions and electrons at the same time, making coincidence measurements possible.

2 VMI Characterisation

The first velocity map spectrometer was designed by Epping and Parker [1] and it focuses the interaction region using three electrodes named repeller, extractor and ground (see fig. 1), each with a voltage V_R,V_E and V_G respectively, where V_G is commonly set to grousnd. The focal distance (i.e. the distance where deblurring is strongest) can then be controlled by varying V_E/V_R and the image size can be adjusted by varying V_E. Here the image size shall be defined as the size a complete image would have on a detector, including electrons or ions emitted perpendicular to the extraction axis (z-axis). This is not to be confused with the size of an image of the interaction region on the detector, which is characterised by the deblurring factor and shall be referred to as *spot size*.
Since the trajectories of particles in a constant electrical field ($\mathbf{E}$) are independent of their mass, in the following mostly electrons will be considered because their time-of-fligh (TOF) spread is much smaller than for heavy ionic fragments. Hence, the extraction axis in the direction of increasing $\mathbf{E}$ is defined as the positive z-direction, thus also defining the elevation (θ) and the azimuth (ϕ). A point on the detector can then be described in terms of the distance from its centre (ρ) and ϕ.

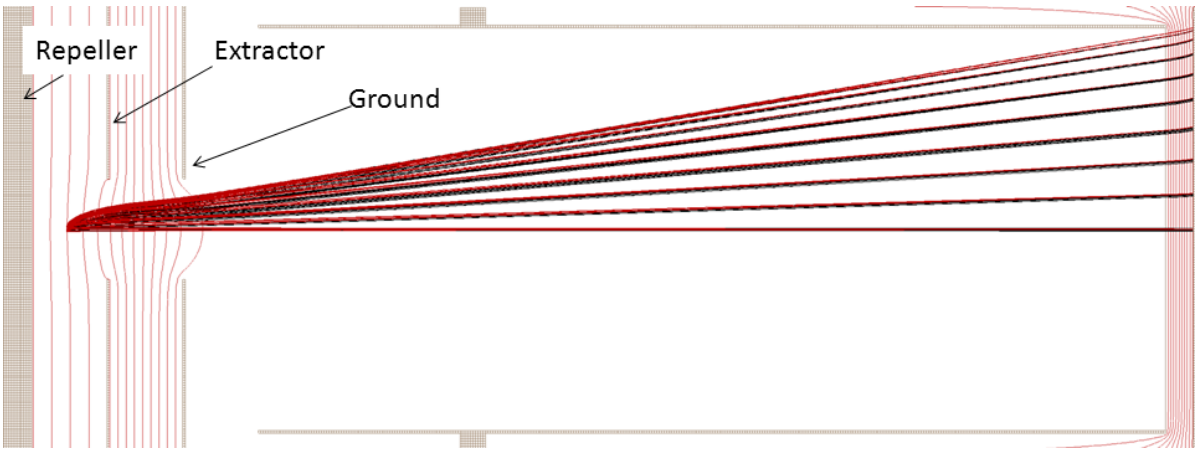

Figure 1: A SIMION simulation of a VMI spectrometer as designed by Epping and Parker [1]. The Electrode spacing is 15 mm and the apertures are 20 mm. Black and red lines are forward and backward emitted electrons respectively, each with a kinetic energy of 100 eV. The initial velocity increases elevation in steps of 10 ° and the voltages on repeller, extractor and ground are -7500 V, -2890 V, and 0 V respectively.

2.1 The CAMP VMI

The VMI spectrometer currently in use [2] can focus on two sides, making it possible to do electron-ion coincidence measurements. For double sided spectrometers like this, the interaction region is usually chosen to be ground and the extractor now also acts as repeller and vice versa. For better optical control it is useful to introduce extra lenses and the drift region now has to be inside a drift tube (DT). The electrodes will be referred to from the centre to the MCP as L1e, L2e,...,DTe for the electron side and L1i, L2i,...,DTi for the ion side, each with a potential V_x. Using the same principles as in the Epping and Parker design, the image size can then be adjusted with V_{DT}, while the focal distance can be controlled by varying V_{DT}/V_{L1}. The potentials of the other lenses can be used to optimise the focusing.
The lens design for the present spectrometer is not mirror symmetric about the xy-plane, causing $\mathbf{E}$ to also be asymmetric (see fig. 2c). This means that the focusing properties are different for ions and electrons, making simultaneous focusing on both sides difficult (but not necessarily worse). In the following only mirror symmetric potential on the lenses will be considered in an attempt to improve comparability. As can be seen from fig. 2b and fig. 2d, there are two major issues for successful VMI focusing. First, the focus plane has to be parallel to the MCP as opposed to the general case, where the focal distance is a function of the emission angle (known as Petzval field curvature). Second, the difference in position of forward and backward emitted electrons with equal but opposite θ (ΔY) on the MCP has to be zero, like it is the case in fig. 1. Additionally, it is desirable to have an image size as large as possible, so in this case this would correspond to a diameter of slightly below 80 mm, the active region of the MCP.
Keeping the image size constant, the VMI performance can then be analysed by looking

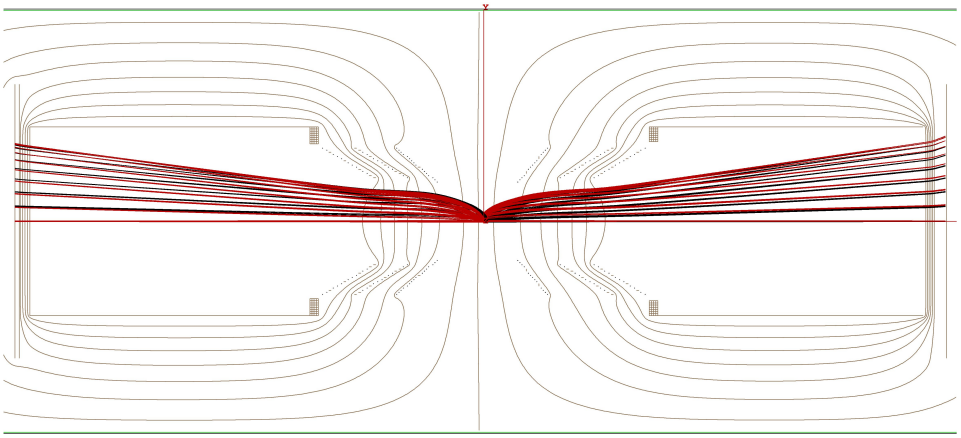

(a) Overview

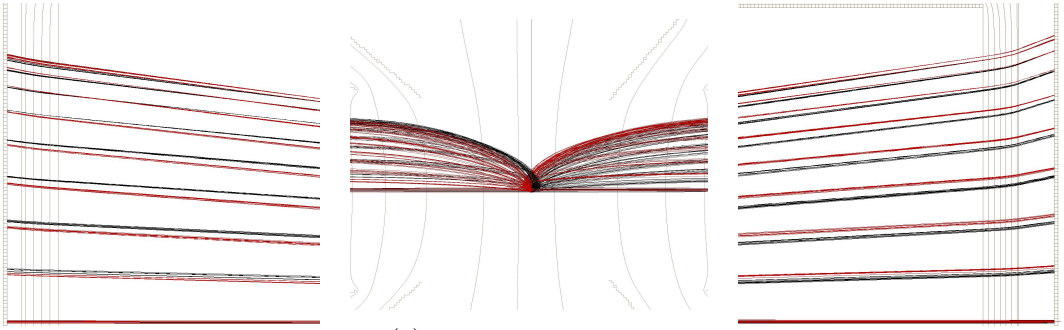

(b) Left MCP (c) Interaction Region (d) Right MCP

Figure 2: A SIMION simulation of the current VMI spectrometer, with the same particle definitions as in fig. 1. The potentials on the electrodes from left to right are -6 kV, -3 kV, -1 kV, 1 kV, 3 kV, and 6 kV and the ions and electrons have initial kinetic energies of 100 eV.

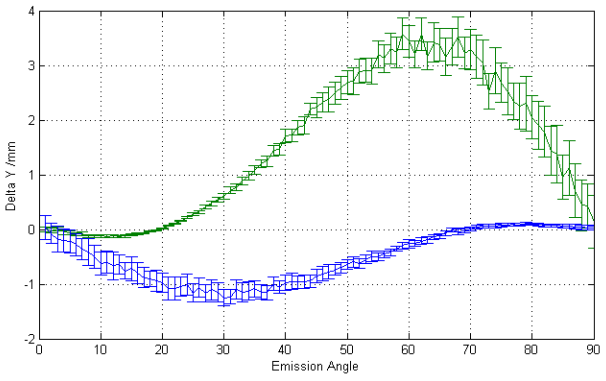

Figure 3: Difference in position on MCP between forward and backward emitted electrons of equal and opposite θ as a function of θ. The error bars represent the spot size on the screen and the simulations were done at V_{L1}=1 kV, V_{L2}=3 kV, and V_{DT}=6 kV (blue) and V_{L1}=0.4 kV, V_{L2}=2.2 kV, and V_{DT}=4.5 kV (green)(asymmetric simulation).

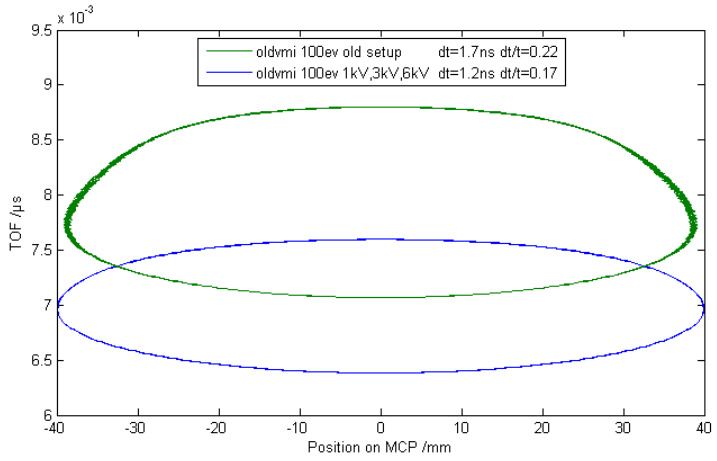

Figure 4: Time-of-flight of electrons at an initial kinetic energy of 100 eV as a function of position on MCP. All electrons were emitted at $\theta = \pi/2$ and the simulations were done at V_{L1}=1 kV, V_{L2}=3 kV, and V_{DT}=6 kV (blue) and V_{L1}=0.4 kV, V_{L2}=2.2 kV, and V_{DT}=4.5 kV (green).

at the spot size and ΔY as a function of θ. In fig. 3, it can be seen that there is a strong correlation between spot size and ΔY. In fact the simulations strongly suggest that wherever ΔY=0 mm, the spot size for the corresponding emission angle is also at a minimum.
Note that with higher V_{L1}, the TOF difference between forward and backward emitted electrons is reduced (see fig. 4), thereby decreasing the temporal resolution. In general, there seems to be a trade-off between spacial and temporal resolution.
Furthermore, since the shape of **E** in the proximity of the interaction region has a large effect on the focusing, it is very difficult to adjust a double sided VMI spectrometer such that it focuses electrons and ions of different kinetic energies at the same time because the potential of the central lenses affect electrons as well as ions and the field is needed to be as symmetric as possible. This symmetry condition also implies that even a fraction of a millimetre in shift of the interaction region can already have a strong effect on the final image. In the case of a mirror symmetric spectrometer this means that the interaction region has to be very close to the centre for good simultaneous focussing on both MCPs.

2.2 The New VMI

The new VMI spectrometer is symmetrical about the xy-plane, which should improve electron-ion coincidence measurements. It uses six lenses, which is meant to improve the control over the shape of the trajectories. Furthermore, the drift tubes are now split into seven rings, making it possible to slow electrons down on their way to the detector (breaking mode) (see fig. 9), as opposed to letting them drift at constant speed (drift

Table 1: Relative potential multipliers for the lenses and DTs

Name	L1	L2	L3	L4	L5
Relative potential	1	2	3	4	5

Name	DT1	DT2	DT3	DT4	DT5	DT6	DT7
Relative potential	10	9	8	7	6	5	4

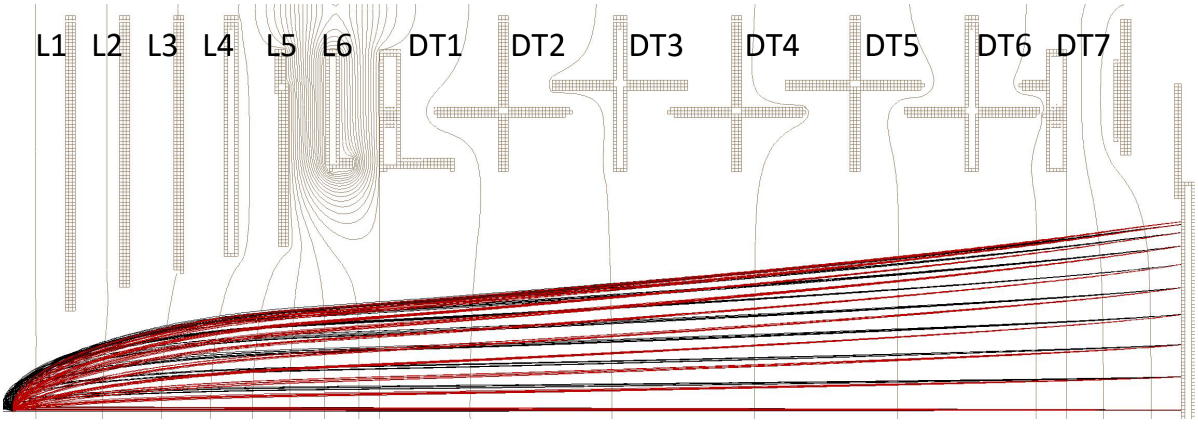

Figure 5: A SIMION simulation of the new VMI spectrometer with the same orbit characteristics as in fig. 1. The relevant potentials are V_{L1}=0.5 kV, V_{L6}=15 kV, and V_{DT1}=5.1 kV. The electrons have a kinetic energies of 100 eV.

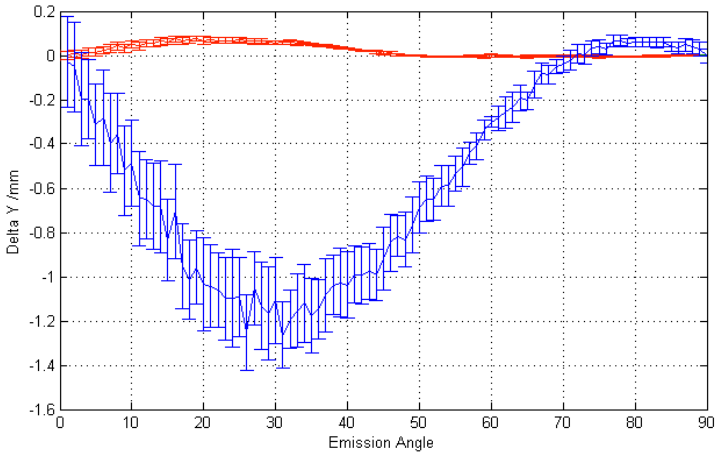

Figure 6: Difference in position on MCP between forward and backward emitted electrons of equal and opposite θ as a function of θ. The error bars represent the spot size on the screen and the simulations are as in fig. 2 (blue) and fig. 5 (red).

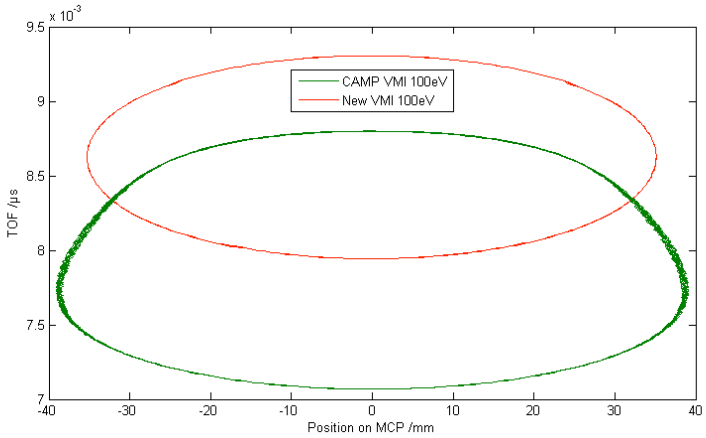

Figure 7: Time-of-flight of electrons at a kinetic energy of 100 eV as a function of position on MCP. All electrons were emitted at $\theta = \pi/2$ and the simulation is one like fig. 5 (red) and a CAMP VMI simulation with V_{L1}=0.4 kV, V_{L2}=2.2 kV, and V_{DT}=4.5 kV (green).

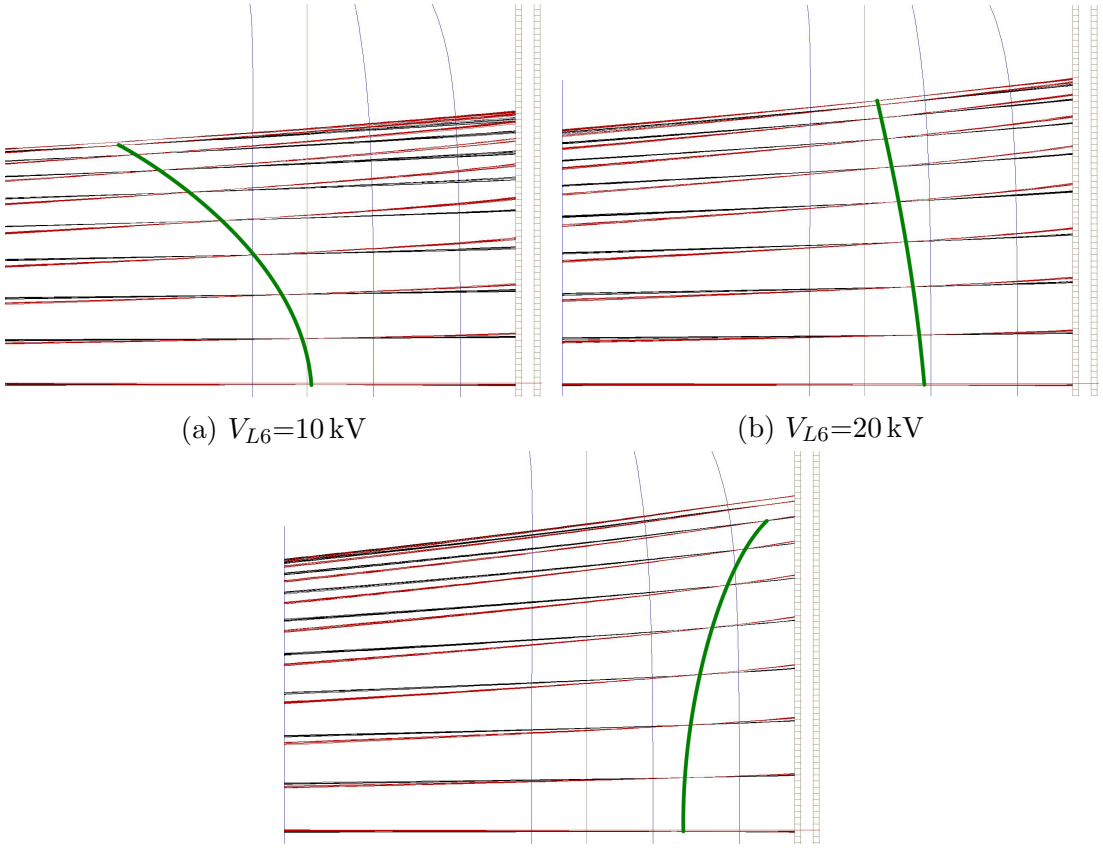

(a) V_{L6}=10 kV

(b) V_{L6}=20 kV

(c) V_{L6}=30 kV

Figure 8: Petzval field curvatures for different V_{L6} (green). The simulations are done for 100 eV electrons with V_{L1}=0.5 kV and V_{DT1}=5.5 kV.

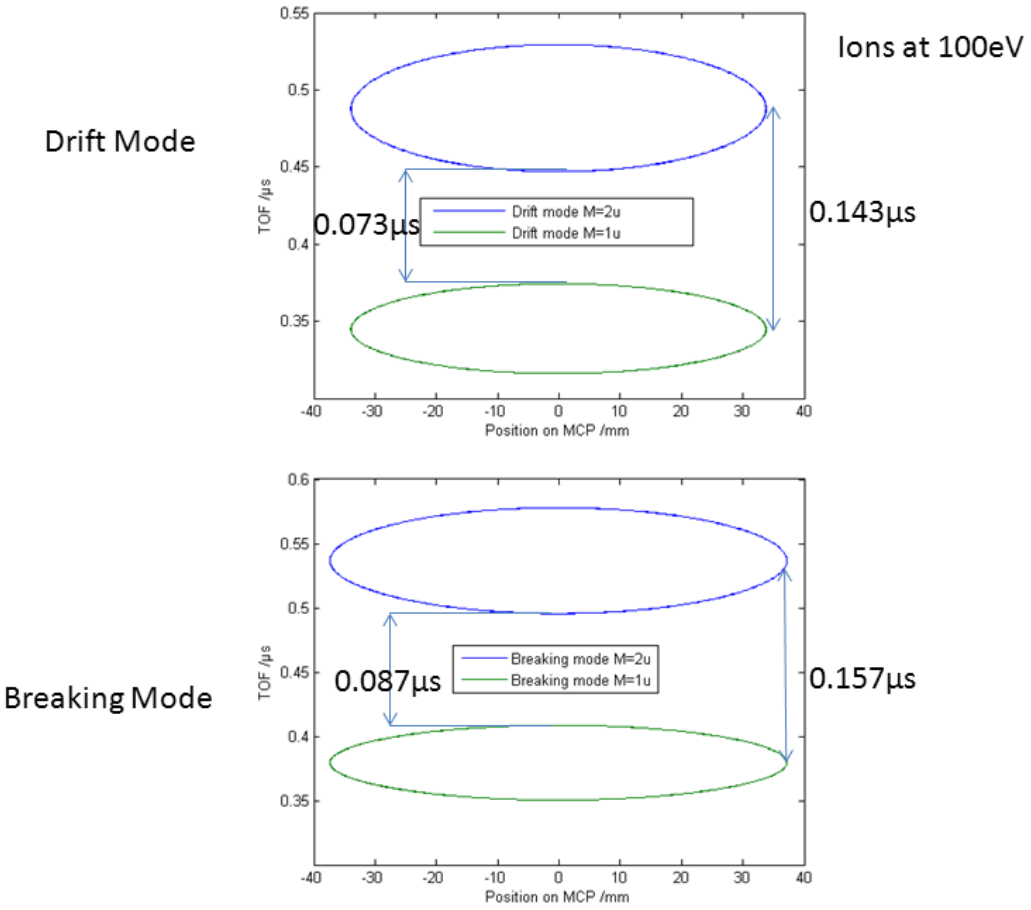

Figure 9: Time-of-flight of electrons at a kinetic energy of 100 eV as a function of position on MCP. All electrons were emitted at $\theta = \pi/2$ and the simulation is one like fig. 5 with ions with a mass of 1 u (green) and 2 u (blue). Simulations were done in drift mode (constant DT electrode voltages) and breaking mode (potentials as in table 1)

mode). Additionally, there is now a mesh between DT and the lenses, which improves the focusing properties considerably but introduces grid distortions.
To simplify operation of the spectrometer, the first five lenses as well as the DTs are intended to have a fixed relation of voltages by connecting them through a resistor chain (see table 1). This way there are three free parameters per side: V_{L1-5}, V_{L6}, and V_{DT1-7}. The image size can be adjusted with V_{DT1}, while the focal distance can be controlled by varying V_{DT1}/V_{L1}. V_{L6} can be used to correct the Petzval field curvature, which requires a comparatively high potential (see fig. 8).
The new spectrometer design offers excellent spatial resolution (see fig. 6), while maintaining a similar temporal resolution (see fig. 7). Note that the increase in ΔY at lower angles hardly decreases the picture quality since low angles correspond to the central region of the MCP, which is generally not of much interest due to high noise levels.

3 Drawings

The CAD drawings for the new VMI spectrometer are based on the dimensions of the CAMP spectrometer. The new spectrometer is intended to be easily exchangeable: the length from end to end is 406 mm, nearly the same as before, meaning that it will work with the same detectors (see fig. 10a).
The DTs are designed with overlapping ledges (see fig. 10b), such that they can still be operated at constant voltage (drift mode) without the possibility of the outside field influencing the electron trajectories. Having theses ledges as far away from the z-axis as possible improves the homogeneity of **E** inside the DTs in breaking mode, preventing unwanted lensing effects.
All the electrodes are held in place by three aluminium rods of 3 mm diameter, isolated using ceramic tubes of 6 mm diameter. Thus there is a distance of 1.5 mm between ground and electrodes, which corresponds to a breakdown voltage of at least 30 kV using alumina. Creeping currents are a also a problem, especially since there are very high voltages intended to be between L5 and L6 which are only 7 mm apart. Using ceramic rings of varying sizes (see fig. 10c), the creeping distance can be increased to 18 mm. Based on the breakdown voltages of the electrodes in CAMP, it can be estimated that L5 and L6 can hold a voltage of over 18 kV.

Table 2: Creeping distances between various electrode pairs.

Electrode pair	L1i/L1e	L1/L2	L2/L3	L3/L4	L4/L5
Creeping distance / mm	20	8	8	8	13
Electrode pair	L5/L6	L6/DT1	DT1/DT2	DT/DT	DT7/rod
Creeping distance / mm	18	18	23	20	8.5

Another critical region is the connection of DT7 to the aluminium rod, which has a creeping distance of 8.5 mm. This restricts the usage of the DT in drift mode, but does not pose a problem in breaking mode, because V_{DT7} does then not reach as high potentials. The relevant creeping distances are summarised in table 2.
The meshes are fixed between two rings that can be seen mounted in front of DT1 in fig. 10c. These rings or *mesh holders* are then attached to the electrodes with three screws. This approach allows the meshes to be removed without having to disassemble anything else, as the mesh holders can simply be pulled out of the spectrometer thanks to the open arrangement of the three aluminium rods (see fig. 10d).

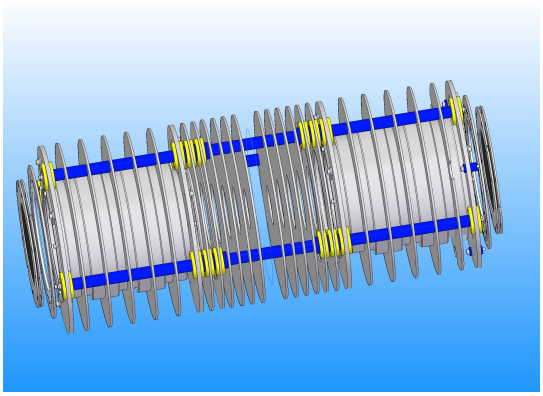

(a) Overview

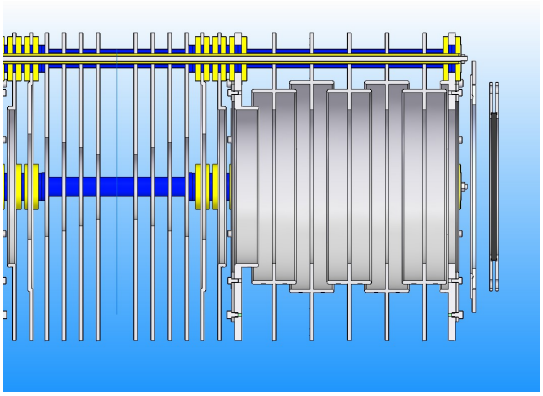

(b) Cutaway view

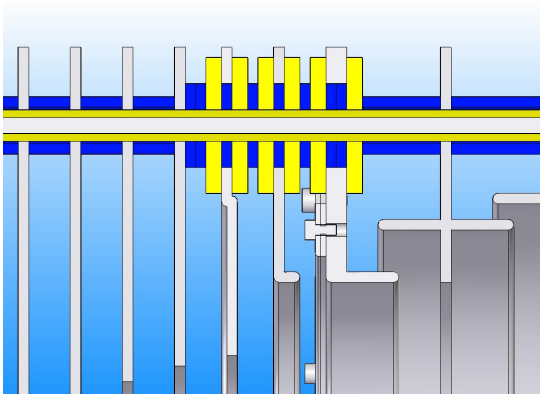

(c) Ceramic isolation

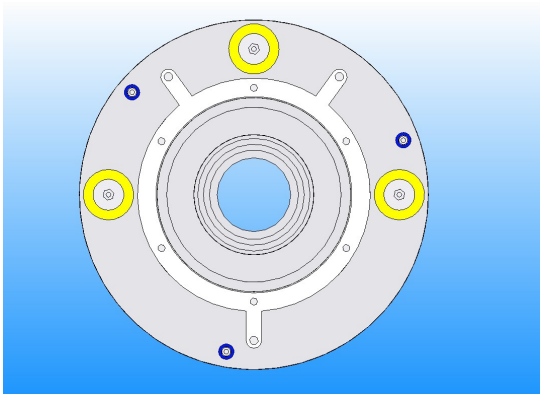

(d) Mesh holder (white)

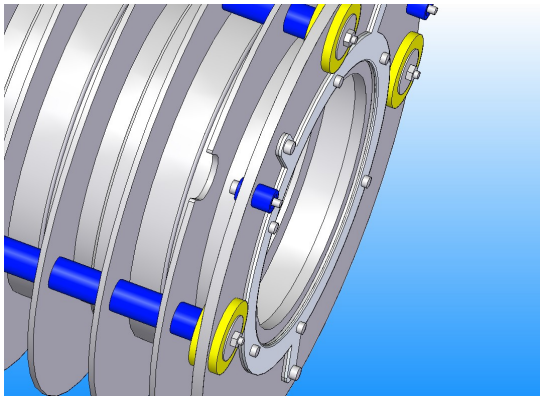

(e) Flange connection

Figure 10: Overview of the new VMI spectrometer design. The MCP is black, ceramics in blue and yellow, and electrodes grey.

4 Systematic Errors

While deblurring yields a sharper image and thus reduces the random error in PAD measurements, other aberrations can remain even in a perfectly focused image, giving rise to systematic errors.

4.1 Angular Pertubations

Since the new spectrometer is held in place be three rods and has several screws for attaching the mesh holders, the entire instrument is not fully cylindrically symmetric. Thus, the electric field acting on an emitted electron would depend on its initial velocities ϕ-component; i.e. electrons with constant kinetic energy won't project a circular distribution onto the MCP. The effect of this asymmetry can be seen in fig. 11 which shows a maximum deviation of nearly 0.5 mm, corresponding to an error in the energy of about 1-3%.
Since this angular dependence of the radius is not mirror symmetric about the xy-plane and is nearly independent of the interaction region's position (see fig. 11b), this shift has to be attributed to the three flange connections at the very end of the spectrometer (fig. 10e). To simplify the simulation as far as possible, better boundary conditions were defined and the three flange connections were removed. The simulation shows a maximum shift of nearly 0.3 mm and is not mirror symmetric about the xy-plane (90° in the fig.12). It seems to be rotated by around 20° and the shift is slightly more pronounced on one side. These effects might be due to incorrect alignment of the interaction region, as well as imperfect symmetry due to the finite size of the voxels. Even given those imperfections in the simulation, there is still a clear pattern visible which roughly matches the symmetry of the spectrometer (taking into account the screws, holders and holes for the rods). As such, it is safe to assume that even minor perturbations from cylindrical symmetry can have a measurable effect on the ion and electron trajectories. The magnitude of this will probably in the range of 0.2-1 % energy shift and hence only relevant for high resolution measurements.

4.2 Pincushion Distortion

With increasing kinetic energy it is to be expected that the measured radius of an image on the MCP can be described with $\rho \propto \sqrt{(KE)}$, where KE is the kinetic energy. Similarly, for electrons with constant KE, the final radius on the MCP should follow $\rho \propto \sin(\theta)$. Both of these relations are not exactly true do to imperfect lensing, leading to so called pincushion distortions. As can be seen in fig. 13, this effect can lead to a shift of about 0.15 mm, causing a systematic error in energy measurements. Here the outer most points on the detector were defined to be correct, causing the shift there to be 0 mm.

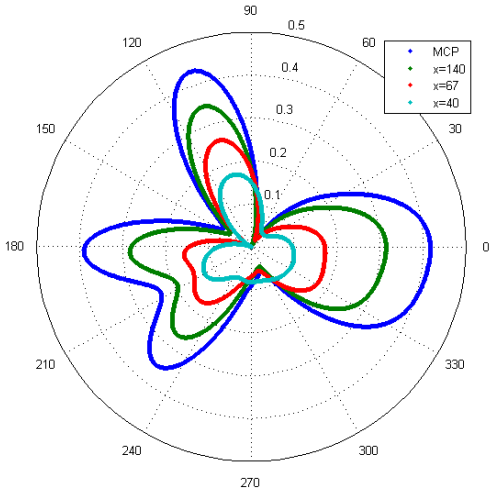

(a) Central interaction region, shift measured at different distances (see (c)).

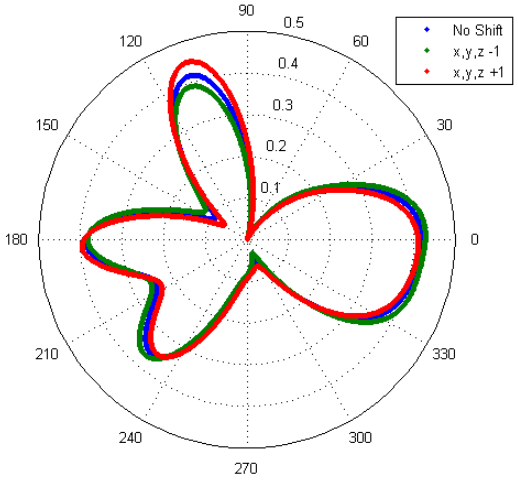

(b) Effect of shifting the interaction region by $\sqrt{3}\,\mathrm{mm}$.

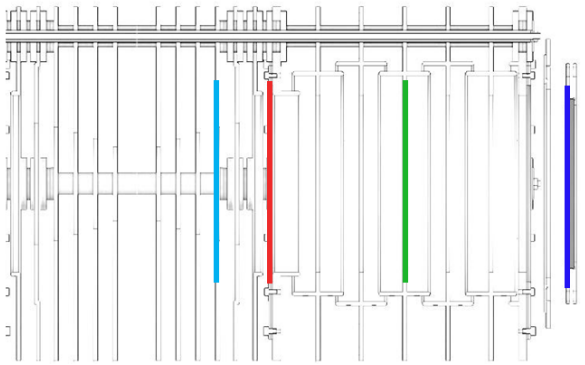

(c) Illustration of the distances at which the data for (a) was acquired.

Figure 11: Simulation of electrons emitted at $\theta = \pi/2$ plotted as a function of ρ against ϕ. For all data points the minimum radius of the otherwise circular projection was subtracted. Measurements were taken at L5 (light blue), in front of the DT (red), inside the DT (green), and at the MCP (blue). The radii for the first three regions are scaled up while the shift for the MCP measurements are in mm. All the simulations were done without the aluminium rods.

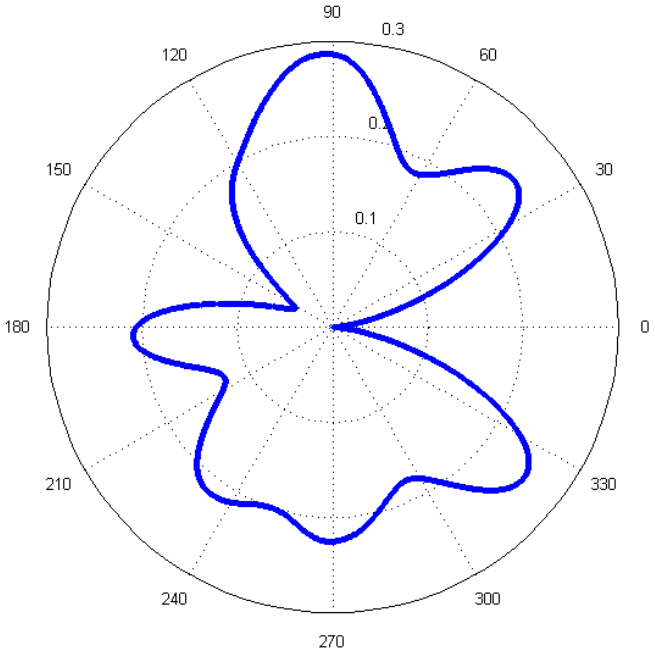

Figure 12: Shift in mm from a perfect circle. The simulation was done in a grounded box with mirror symmetry about the xy-plane, corresponding to the 90° direction in this plot.

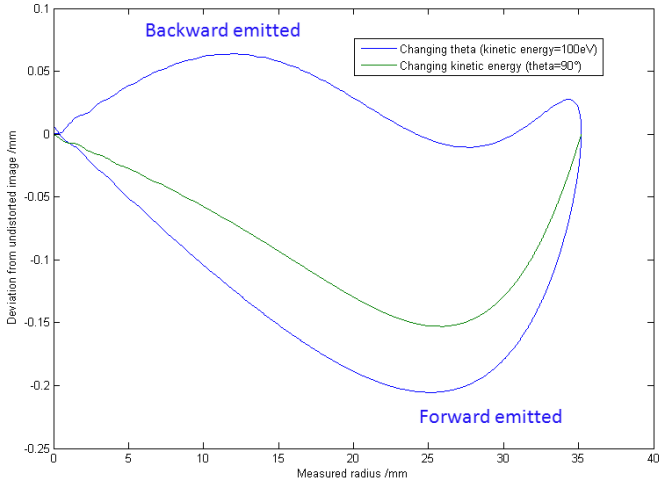

Figure 13: Shift of measured radius as a function of the measured radius. Simulations were done over a range of kinetic energies between 0 eV and 100 eV (green) and over a range of initial velocity elevation between 0° and 180° (blue).

References

[1] A. T. J. B. Eppink, D. H. Parker, *Velocity map imaging of ions and electrons using electrostatic lenses: Application in photoelectron and photofragment ion imaging of molecular oxygen*, Rev. Sci. Instrum. **68** (1997)

[2] L. Strüder et al., *Large-format, high-speed, X-ray pnCCDs combined with electron and ion imaging spectrometers in a multipurpose chamber for experiments at 4th generation light sources*, Nucl. Instr. and Meth. in Phys. Res. A **614** (2010)